Social synchronisation of brain activity by eye-contact

Caroline Luft (c.luft@qmul.ac.uk)
Queen Mary University of London
Ioanna Zioga
Radboud University
Anastasios Giannopoulos
National Technical University of Athens
Gabriele Di Bona
Queen Mary University of London
Andrea Civilini
Queen Mary University of London
Vito Latora
Queen Mary University of London https://orcid.org/0000-0002-0984-8038
Isabelle Mareschal
Queen Mary University

Article

Keywords: eye contact, brain activity, brain networks, social synchronisation

Posted Date: July 12th, 2021

DOI: https://doi.org/10.21203/rs.3.rs-654192/v1

Version of Record: A version of this preprint was published at Communications Biology on May 4th, 2022.
See the published version at https://doi.org/10.1038/s42003-022-03352-6.

Social synchronisation of brain activity by eye-contact

Luft, CDBL[1]*, Zioga, I[1,2], Giannopoulos, A[3], Di Bona, G[4], Binetti, N[1], Civilini, A[4], Latora, V[4,5,6,7], Mareschal, I[1]
*corresponding author (c.luft@qmul.ac.uk)

Affiliations:

[1] School of Biological and Chemical Sciences, Queen Mary, University of London, London E1 4NS, United Kingdom

[2] Donders Institute for Brain, Cognition and Behaviour, Radboud University, Nijmegen, The Netherlands

[3] School of Electrical and Computer Engineering, National Technical University of Athens (NTUA)m Athens, Greece

[4] School of Mathematical Science, Queen Mary University of London, London E1 4NS, United Kingdom

[5] Dipartimento di Fisica ed Astronomia, Università di Catania and INFN, I-95123 Catania, Italy

[6] The Alan Turing Institute, The British Library, London NW1 2DB, United Kingdom

[7] Complexity Science Hub, Josefstäadter Strasse 39, A 1080 Vienna, Austria

Abstract

Humans make eye-contact to extract information about other people's mental states, recruiting dedicated brain networks that process information about the self and others. Recent studies show that eye-contact increases the synchronization between two brains. We investigated how eye-contact affects the frequency and direction of the synchronization within and between brains and the characteristics of the dual brain network (i.e. hyperbrain). Eye-contact was associated with higher coherence in the gamma frequency band (30-45Hz) for between and within brain connections. Network analysis revealed that some brain areas served as hubs which linked within- and between- brain networks (midparietal, midfrontal and right parietal areas). Friends showed more efficient eye-contact hyperbrain networks than strangers. During eye-contact, some dyads spontaneously adopted leader/follower roles, resulting in an increase in synchronization from leader to follower (interbrain) in the alpha frequency band. Eye-contact affected directed and undirected synchronization between brains more than within brains, offering support to the interactive brain hypothesis.

Introduction

Human and non-human primates' gaze is drawn to other's eyes[1,2]. However, while non-human primates have a pigmented sclera, human sclera are white[3]. This morphological difference allows humans to extract a wealth of information from our conspecific's eyes, which may shape our social interactions. For instance, humans can detect eye-contact from a longer distance than non-human primates[4] and use this information to infer other people's mental states and intentions (for a review[5]). The brain regions involved in eye-contact overlap with structures in the *social brain network*[6], including ventral and medial prefrontal cortex, superior temporal gyrus, fusiform gyrus, cingulate gyrus and amygdala (for a review[7]), suggesting that mutual eye-contact is key for inferring others' emotions and intentions. The perception of direct eye-contact in humans is consistently found to involve the superior temporal sulcus (STS)[8–10], a region which is a key part of the *mentalising* network that is involved in tasks that require

making inferences about the mental states of others[11]. Research has made remarkable progress towards understanding how eye-contact is processed in a single (perceiver's) brain, but eye-contact is an interactive process between two people. More recently, we have begun to extend this understanding to multiple brains – for example, the synchronization of activity between two brains has been found to increase during eye-contact[12–14]. However, we still do not know how both intra and inter brain activity is integrated, nor the functional role of this synchronised activity.

To address this, it is important to examine the activity of two brains simultaneously, through a process known as *Hyperscanning*[15–17]. Hyperscanning studies have shown that higher synchronization between brains (e.g. interbrain activity) is associated with more effective social interactions[18–29]. For example, higher synchrony between teacher's and student's brains was found to be associated with better learning[19,22,23]. Groups with higher interbrain synchrony are more likely to be cooperative but also more likely to be hostile towards members of other groups[30]; interbrain synchrony was also higher during positive emotional interactions between parents and infants[25] and associated with better emotional regulation of both the child and parent[24]. It was also found that higher synchronization between people's right temporo-parietal junction was associated with enhanced team collaboration[31]. The right lateralisation of the synchronisation effects was also observed in romantic partners when cooperating[32].

Interestingly, this synchronization between brains may be directed (e.g. from one brain to the other), especially in leader-follower scenarios[33–35], a phenomenon also demonstrated in non-human animals[36]. For instance, a study on three-group discussions in which a spontaneous leader emerged observed higher synchronization between the brains of the leader and the follower compared to between the followers[33]. Another study[34] demonstrated that leaders presented stronger motor-related oscillatory patterns compared to followers when interacting in a finger tapping task. A computational modelling study[37] explained this effect by demonstrating that successful behavioural interaction requires an increase in between-unit coupling (e.g. interbrain) and a decrease in within-unit (e.g. intrabrain) coupling. For instance, they observed that leader-follower interactions require the follower to have low within-unit coupling whereas the relationship between two leaders tends to result in low between unit coupling. Altogether, these studies suggest that individual brains' responses might affect the dynamic of interactions, these dynamics can also affect the individual brains responses. These findings highlight the need to understand how interactions work in the dual brain system, combining both inter and intra brain connectivity. Since eye-contact is a key factor in initiating and coordinating human interactions, it is important to determine if eye-contact alone (a) plays a role in establishing leader-follower dynamics, and (b) results in directed synchronisation between brains, for instance, from leader to follower.

Graph theory can be used to quantify the properties of entire networks with measures that estimate how information flows through them based on their nodes (i.e. brain areas) and edges (i.e. connections)[38]. A few studies have exploited graph theory to understand the global and local characteristics of the so-called *hyperbrain* networks which include both intra and interbrain connections[39–41]. For example, a study[41] observed that the brain networks of an uncooperative dyad (two defectors in a prisoners' dilemma game) contained less interbrain links and was more modular (i.e. stronger connectivity within brains than between brains). The current study aimed to investigate the hyperbrain networks during eye-contact and to reveal their functional meaning by comparing the network properties of friends vs. strangers (i) and of spontaneously emerging leader-followers (ii). The latter evaluated whether synchronization would occur from leader to follower in a dual eye-tracking time reproduction task (Fig.1A).

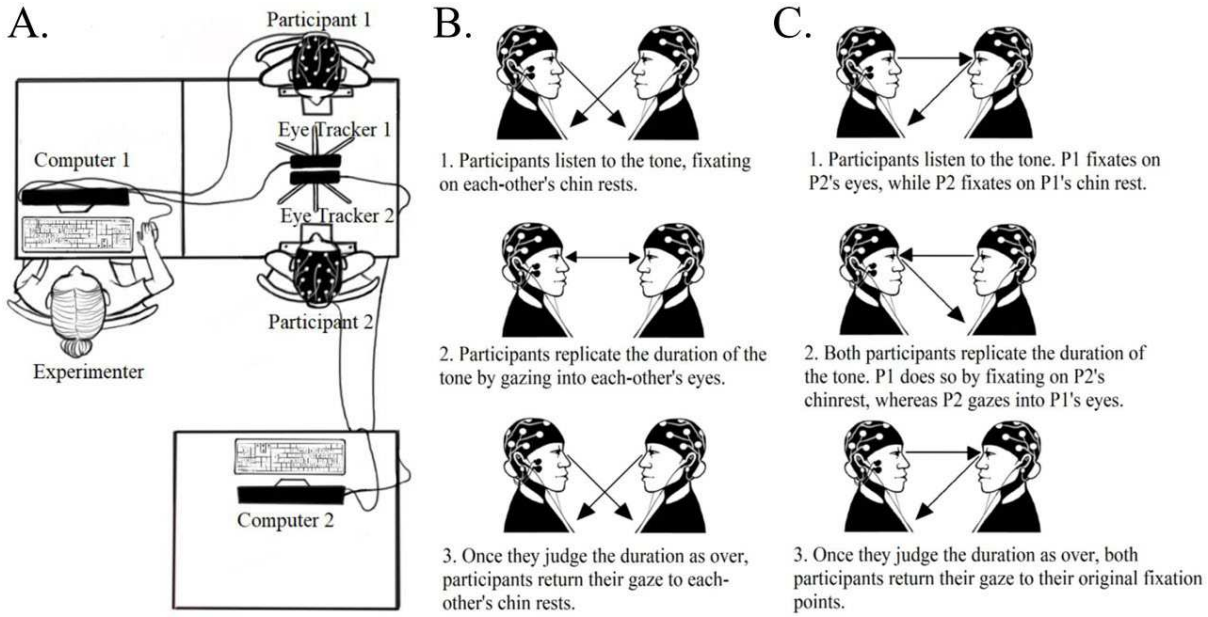

Fig.1. Experimental setup and task. A. Two computers were synchronized during the experiment and each computer collected EEG and eye-tracking data from one participant but received EEG and eye-tracking event markers with no delay (all hardware was centrally controlled through Matlab). **B. Eye contact time estimation task**: participants faced each other and were required to reproduce the duration of a tone delivered through headphones without speaking to their dyadic partner. **Eye-contact condition:** during the delivery of the tone, participants were instructed to fixate on a sticker on the other participant's chinrest. After the tone ended, the participants were instructed to look at other's eyes for the duration of the tone, looking back down to indicate that they finished reproducing the tone duration. The tone the participant heard was either long (2.5s) or short (1.5s) and in some trials, the participants heard different tone durations. **C. Non eye contact control condition**: participants replicated the duration of the tone but never made eye contact. Participant A listened to the tone while fixating on their partner's eyes while participant B listened to the tone while fixating on their partner's chinrest. After the tone, both participants replicated its duration, participant A by fixating their partner's chinrest and participant B by fixating their partner's eyes. To indicate the end of the tone interval, each participant reverted their gaze back to the starting position. In one block, participant A replicated the duration by looking in their partners' chinrest and the other by looking at the participant B's eyes (while participant B looked down to the chinrest), and in the other block, the roles reversed. The analysis of connectivity was restricted to the data from the period where both participants were performing the time reproduction task (step 2 of Fig.1B and C). *Drawing credits to* Tatiana Adamczewska.

The time reproduction task enabled us to measure interbrain synchronization (EEG) during short time intervals while the participants engaged in a task, for bouts of eye-contact similar in duration to those people usually engage in during a face-to-face interaction[42]. Considering the individual differences in relation to preferred eye-contact duration, we chose time intervals of 1.5s and 2.5s which are within the durations found to be comfortable for people[43]. The high time resolution of EEG enabled us to measure phase synchronization during these short bouts of eye-contact. Our behavioural results (*Supplementary Results S1*) showed that people truly engaged with the time reproduction task, reproducing lower durations following short intervals and longer durations following longer intervals (Fig.S1A). Our behavioural results showed that: 1) participants underestimated durations during mutual eye-contact compared to the control condition; and 2) during eye-contact, the estimated durations

changed according to their partner estimations, which was evidenced by a correlation between the pair's estimations (Fig.S1B). Furthermore, we found that in some pairs, one participant consistently gazed down first during the eye-contact condition, while the other participant followed, and this was not the result of one person simply responding earlier than the other (*Supplementary Results S2*). We considered the participant who gazed first to be the leader and the one who followed to be the follower, roles that were used to investigate directed connectivity. The association between gaze following behaviour and leadership has been observed in both non-human[44] and human animals[45], and in this study, we investigated whether the direction of the synchrony between brains changes according to people's leader/follower roles.

Considering the complexity of this dataset, we implemented a two-step approach for both undirected (coherence) and directed (phase slope index) synchronization measures. Coherence provides a measure of instantaneous phase synchronization, therefore undirected, whereas the phase slope index provides a measure of non-instantaneous phase synchronization (small time delay), therefore directed (i.e. the phase of one signal precedes that of the other). We first compared the connectivity during eye-contact vs. control using a non-parametric cluster permutation approach (see Methods). This enabled us to identify a frequency band to conduct the network analysis. We then looked at the network characteristics considering both inter and intra brain connections as a single network and examined if they differed between friends and strangers and if they were directed from leader to follower.

Results

Undirected connectivity: *Interbrain coherence during eye-contact*

A nonparametric cluster permutation procedure revealed a significant cluster in the gamma frequency band (30-45Hz) with higher interbrain synchronization during eye-contact compared to the control task (Fig.2). The cluster had 22 significant links, mainly between the partners' right hemispheres (*cluster t-statistic* = 60.9, *t-critical* = 16.6, $p = .029$). The analysis of the topography of the interbrain connections shows that the highest differences in coherence during eye-contact compared to control were in the right parietal area (including midline, Fig.2B). The direct comparison of gamma coherence in the identified cluster confirmed the presence of significantly higher coherence during eye-contact compared to control ($t(49) = 3.419$, $p < .001$, Fig.2C). There were no significant clusters in any other frequency band ($p > .1$).

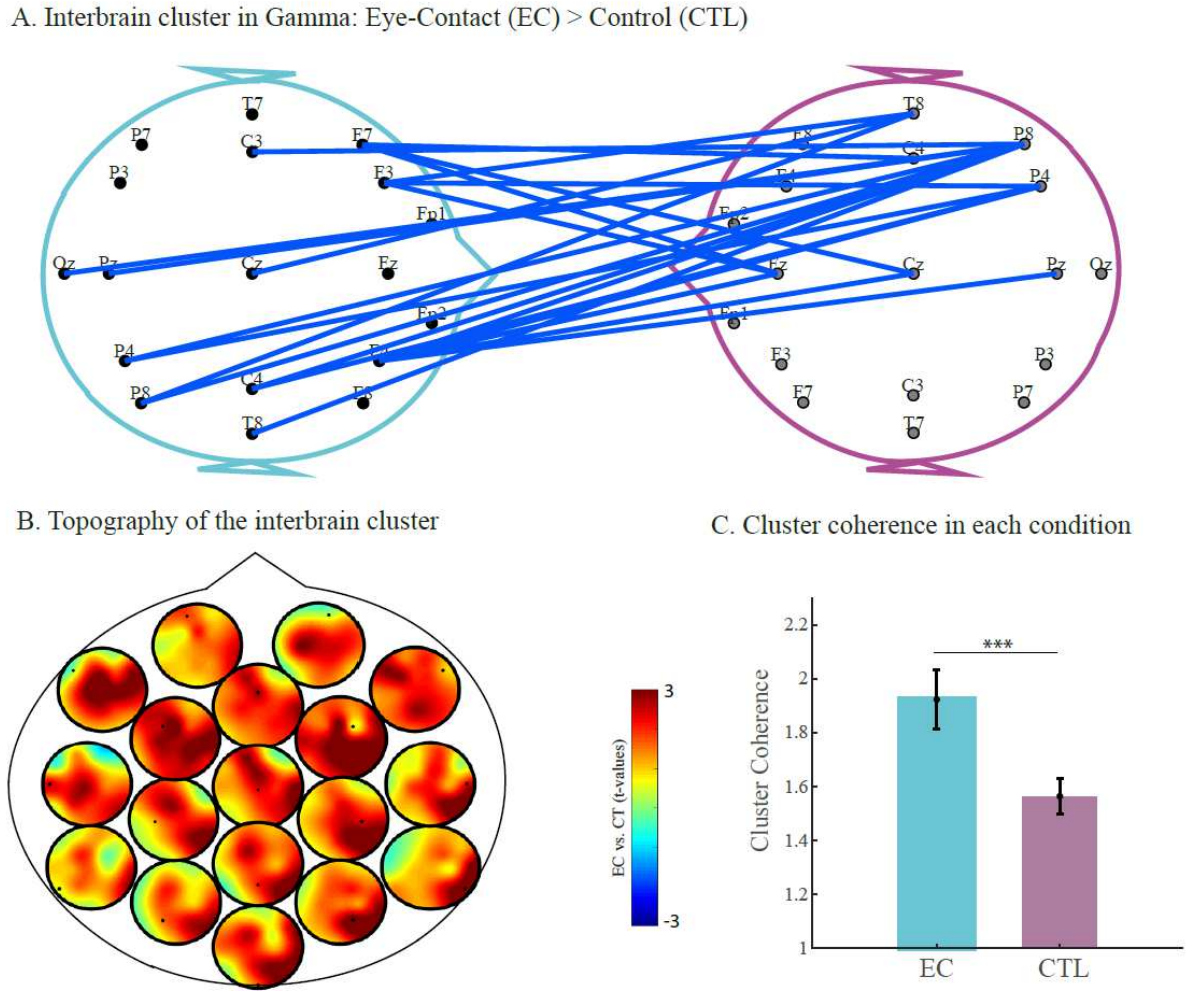

Fig.2: Interbrain synchronization during eye-contact. Gamma-band brain synchronization (coherence) within pairs during eye-contact (EC) vs. control condition (CTL). **A.** Blue lines represent electrode pairs with significantly higher gamma coherence in EC vs. CTL. The significant cluster shows widespread connections between brains, especially distributed on the right hemisphere. **B.** Heads-in-head representation of the difference in gamma coherence during eye contact compared to the control task for the interbrain connections. Each circle represents the scalp topography of the connections with the channel highlighted inside as a black dot. Red colours represent an increase in coherence between that channel (dot) and the other person's scalp during eye contact expressed as a t-value of the contrast through the cluster permutation analysis. Red colours represent higher t-values for coherence during eye-contact compared to control. **C.** Average coherence for the cluster of interbrain connections during eye-contact and during the control task. Error-bars represent ± 1 SEM. *** $p < .001$.

Intrabrain coherence during eye-contact

We also looked at the differences in intrabrain coherence during eye-contact compared to the control task. A nonparametric cluster permutation approach was conducted to compare the intrabrain coherence networks between conditions. We observed a significant positive cluster (*cluster t-statistic* = 52.18, *t-critical* = 25.65, $p = .030$) with higher coherence in gamma frequency band during eye-contact (compared to control) with connections mostly on the right hemisphere (Fig.3).

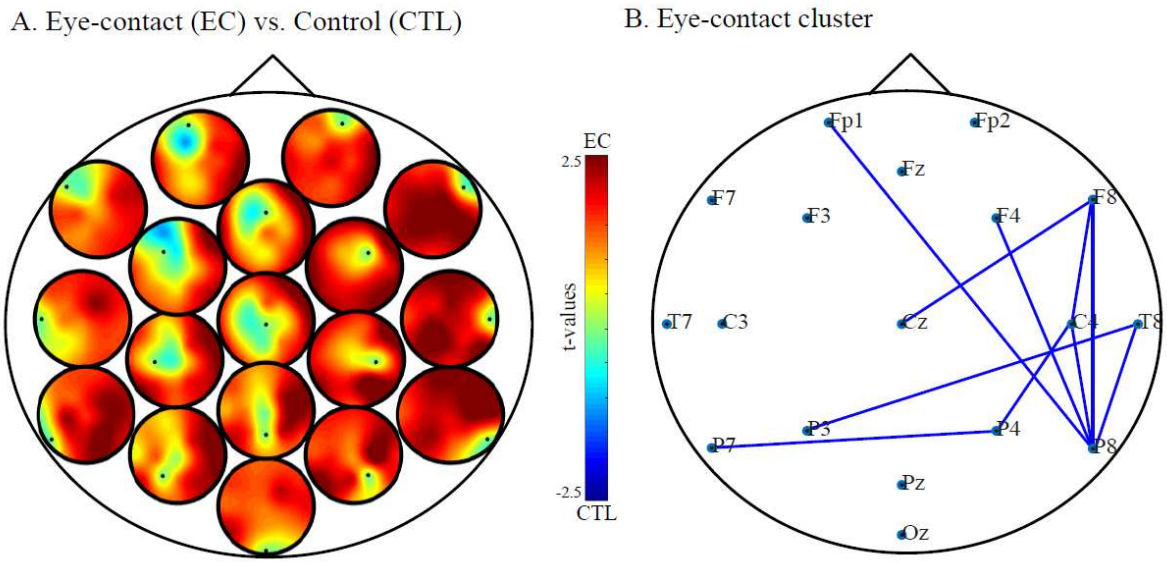

Fig.3: Intrabrain synchronization during eye-contact. Significant cluster of intrabrain connectivity during eye-contact (EC) compared to no eye-contact (CTL). **A**. Heads-in-head representation of the difference in gamma coherence during eye contact compared to the control task. Each circle represents the topography of the connections with the channel highlighted inside as a dark dot. Red colours represent an increase in coherence during eye contact expressed as a t-value of the contrast as conducted in the cluster permutation analysis. **B.** Significant connections in the observed cluster. Most significant connections are between right parietal and the rest of the brain

Undirected Network Analysis: Friends vs. Strangers

Since we observed that eye-contact was associated with increased coherence in the gamma band for both inter and intrabrain connections, we analysed the global and local network properties of the gamma band networks using graph theory measures. To uncover the functional significance of the undirected connections, we compared the network characteristics of pairs of friends vs. strangers (see Methods for descriptions of all measures extracted from the network analysis).

We focused on the network characteristics during eye-contact using the control task as a baseline. For each pair, we calculated the z-scores of each edge based on the mean and standard deviation of gamma coherence in the control condition and thresholded the matrix for each pair. Despite having higher absolute values, intrabrain connections showed significantly lower z-scores than interbrain connections ($t(99) = 6.879, p < .001$). This shows that in general, making eye-contact is associated with higher increases in synchronization between brains (interbrain) compared to the connections within a brain (intrabrain), as shown in Fig.4A. We also asked whether friends would show higher changes in overall coherence strength during eye-contact. We applied a 2 (*edge_type: inter vs. intra brain)* x 2 (*friendship: friends vs. strangers*) mixed-design ANOVA on the average strength (mean z-scores - all electrodes). We observed that *interbrain* connections increased significantly more during eye-contact compared to the *intrabrain* connections ($F(1,98) = 13.183$, $p < .001$, *partial* $\eta^2 = .119$). There was also a main effect of *friendship* ($F(1,98) = 7.227$, $p = .008$, *partial* $\eta^2 = .069$) and a significant interaction between *edge type* and *friendship* ($F(1,98) = 4.168$, $p = .044$, *partial* $\eta^2 = .053$). Pairwise contrasts showed that friends had significantly stronger *interbrain* connections than strangers ($t(98) = 2.439$, $p = .017$), but not *intrabrain* connections ($t(98) = 1.597$, $p = .114$). Similarly, friends showed significantly higher interbrain compared to intrabrain connections ($t(45) = 5.274$, $p < .001$), which was also significant for strangers ($t(53) = 3.292$, $p = .002$).These analyses reveal that making eye-contact affects the general strength of the

interbrain connections more than the intrabrain ones, and that interbrain synchronization during eye-contact is higher in friends compared to strangers.

To investigate the network characteristics relative to the baseline (control task), we calculated the following network measures: density (proportion of connections, intra and interbrain), global and local efficiency, modularity and rich club coefficient (Fig.4B). For all the network analyses, we excluded the pairs which did not show interbrain edges during eye-contact (6 pairs out of 50 were excluded, 3 pairs of friends and 3 pairs of strangers). We conducted a 2 (*edge type: intrabrain vs. interbrain)* x 2 (*friendship: friends vs. strangers)* mixed design ANOVA on the density. We observed a higher density for interbrain compared to intrabrain connections ($F(1,86) = 51.040$, $p < .001$, *partial* $\eta^2 = .372$), a significant effect of *friendship* ($F(1,86) = 9.521$, $p < .001$, *partial* $\eta^2 = .100$) and a significant interaction between *edge type* and *friendship* ($F(1,86) = 5.003$, $p = .028$, *partial* $\eta^2 = .055$) since the networks of friends showed a significantly higher interbrain density compared to strangers ($t(86) = 2.825$, $p = .006$), but similar intrabrain density ($t(86) = 1.399$, $p = .166$). Interbrain density was higher than intrabrain density for friends ($t(39) = 6.470$, $p < .001$) and strangers ($t(47) = 3.586$, $p < .001$). Networks of friends showed slightly higher global efficiency ($t(42) = 2.139$, $p = .038$) and local efficiency ($t(42) = 2.071$, $p = .045$), but no difference in modularity and assortativity ($p > .1$, Fig.4B). The averaged (and thresholded) connectivity matrix for friends and strangers (Fig.4C) demonstrated a larger number of interbrain connections between friends (Fig.4C-left) compared to strangers (Fig.4C-right).

To test if the networks have higher connectivity in specific areas, we grouped the electrode data into 8 regions of interest (ROIs Fig.4D): right frontal (RF: F4, F8, Fp2), right parietal (RP: P8, P4), left frontal (LF: Fp1,F7,F3), left parietal (LP: P3,P7), right centro-temporal (RCT: C4, T8), left centro-temporal (LCT: C3, T7) midfrontal (MF: Fz, Cz) and midposterior (MP: Pz, Oz). We averaged the degree (number of connections), and local and global efficiency for each ROI considering the entire network (intra and interbrain connections). We conducted a 2 (*friendship: friends vs. strangers*) x 8 (*ROI: LF,RF,LP, RP, MF,MP,RCT,LCT*) mixed-design ANOVA on each of these dependent variables (degree, local, and global efficiency). We observed that both degree and global efficiency were higher in the midfrontal and midposterior regions and lowest at the frontal regions bilaterally. Although there was a main effect of friendship, it did not interact with ROIs, which suggests that friends and strangers showed a similar network structure (Supplementary Results S3). Regarding average local efficiency, we also observed a significant effect of *ROIs* ($F(7,602) = 47.824$, $p < .001$, *partial* $\eta^2 = .357$), a main effect of *friendship* ($F(1,86) = 6.410$, $p = .013$, *partial* $\eta^2 = .069$), and an interaction between *ROIs* and *friendship* ($F(7,602) = 2.982$, $p = .004$, *partial* $\eta^2 = .034$). Pairwise comparisons (Fig.4D) between ROIs showed that the midposterior region exhibited higher local efficiency than all the other regions ($p < .05$), followed by the midfrontal region which was also higher ($p < .05$) than all others (except midposterior). The frontal areas (left and right) showed the lowest local efficiency compared to all others ($p < .001$), but they did not differ between each other. To understand the interaction, we conducted a repeated measures ANOVA for the local efficiency between the 8 ROIs. We observed a stronger effect of ROI for strangers ($F(7,329) = 33.089$, $p < .001$, *partial* $\eta^2 = .413$) than for friends ($F(7,329) = 13.370$, $p < .001$, *partial* $\eta^2 = .255$) as strangers showed a very low local efficiency over the frontal regions and slightly lower towards the right (Fig.4D).

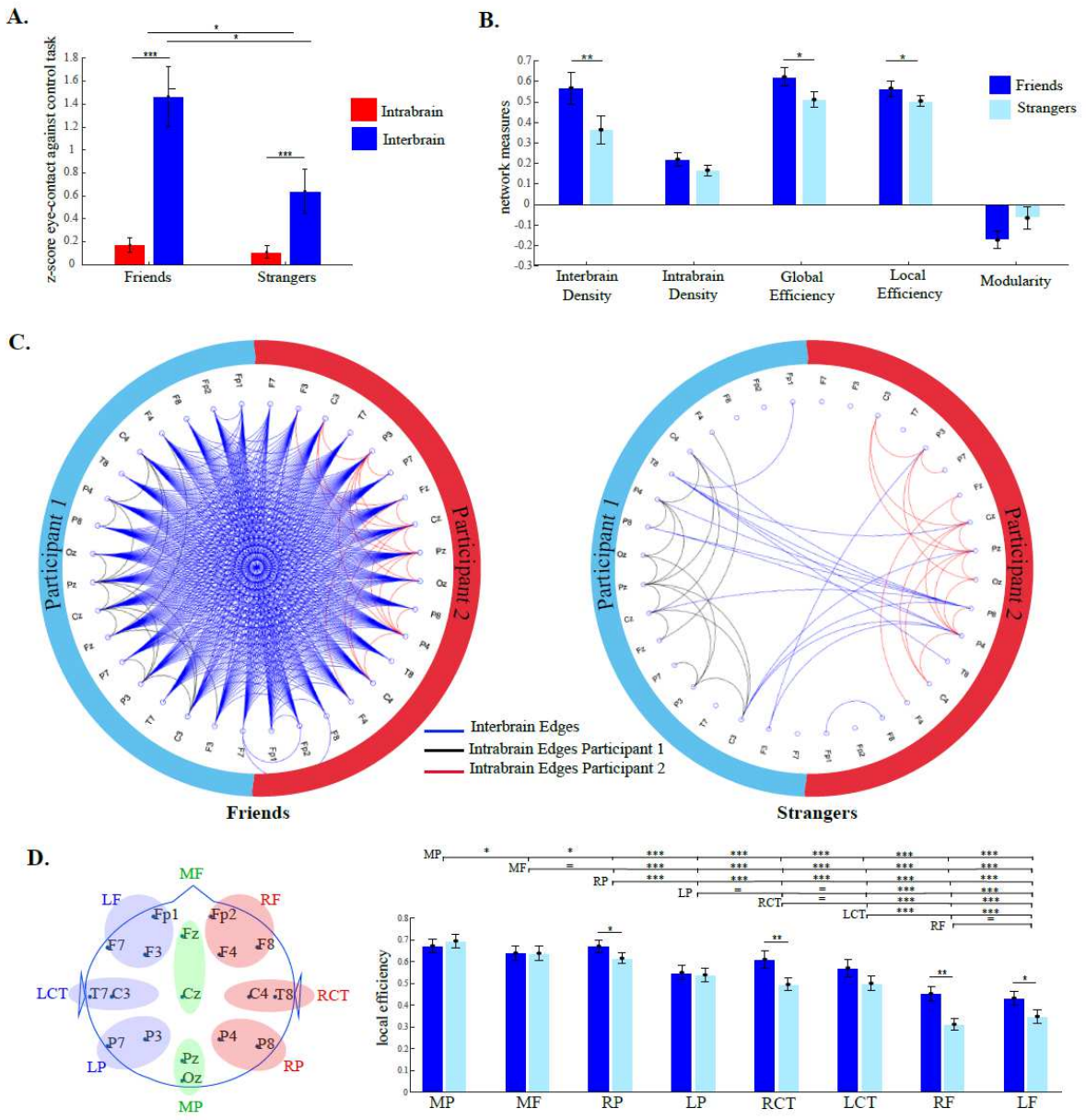

Fig.4. Hyperbrain network during eye-contact. **A.** Intra (red) and interbrain (blue) connectivity strength of friends and strangers measured as average of z-scores during eye-contact against control. **B.** Network measures of friends (dark blue) and strangers (light blue) during eye-contact. These measures are based on the binary coherence networks. **C.** Coherence networks during eye contact, the edges represent the coherence values which increased on average by more than 1SD against the control task for friends (left) and strangers (right). Interbrain edges are represented in blue, intrabrain edges of participants 1 are in black and 2 are in red. To improve visualisation of the key areas further, we also thresholded the averaged interbrain connections at 2SD for friends and strangers separately. This procedure resulted in no edges for the strangers, but in a number of connections for friends, especially in the right temporo-parietal region (Fig.S3A). **D.** Local efficiency of each ROI (left hand side): MP: mid posterior; MF: midfrontal, RP: right parietal, LP: left parietal, RCT: right centro-temporal; LCT: left centro-temporal, RF: right frontal, LF: left frontal. Error bars represent ±1 SEM. *** $p < .001$/** $p < 0.01$/ * $p < .05$.

We investigated whether the networks showed a rich-club configuration. We calculated the rich-club coefficient for each pair's network and considered the structure as rich-club (see Methods). We found evidence of rich-club structure in 38 out of the 44 pairs (86.4%). From all friends, 16 pairs presented a rich-club structure (80% of the friend pairs) whereas 22 pairs of strangers (91.7%) presented such a structure (*chi-square* = 1.261, p = .261). This shows that there was no significant difference in the rich-club structure between these groups. For each of the pairs who presented a rich-club structure, we calculated the proportion of times each node was a rich-club (Fig.S3C) against all the pairs who showed a rich-club structure. This analysis showed that the key channels to show a rich club structure were the midline parietal (Pz), followed by the right parietal (P4) and midline central (Cz). The channels which were less likely to be hubs were the frontal areas (bilaterally). These findings suggest that the midline and right parietal regions might serve as hubs which integrate internal and external connections during eye-contact.

Directed Connectivity Analysis: *Leaders vs. Followers*

We adopted the same approach to examine whether the connectivity was directed during eye-contact, between brains (e.g from leader to follower) and within brains. As explained in the methods, the phase slope index (PSI) indicates whether the phase of a signal precedes the phase of the other signal in each frequency band. If there is a leader-follower effect, we expect the phase of the leader to precede the phase of the brain signals of the follower.

Interbrain directed connectivity

Our behavioural analysis revealed that in some pairs, one participant consistently gazed down first, henceforth referred to as the leader of the pair, and for this analysis we only used pairs with strong leadership indices (*Supplementary S2*). We adopted a nonparametric cluster permutation considering the direction of the connection (from leader to follower) separately and the condition which showed stronger connectivity values (eye-contact vs. control). This enabled us to use the same cluster analysis approach we adopted for analysing coherence. This approach enabled us to define the prominent frequency of the network, both for interbrain and intrabrain connections.

We observed a significant interbrain cluster in the alpha frequency band (Fig.5A) during eye contact from leader to follower (*cluster statistics* = 43.35, *t-critical* = 27.33, p = .0278). Fig.5B illustrates the full topography of all the directed connections from leader to follower during eye-contact and during the control task. During eye-contact (compared to the control task), the synchronization flux was from leader to follower, with the right hemisphere regions leading the frontal and midline areas of the follower. Directed phase synchronization in this cluster from leader to follower was positively correlated with leadership strength during eye contact (r = .508, p <.001), but not during the control task (r = -.265, p = .066). There was no cluster in the opposite direction (from follower to leader) nor clusters showing higher synchronization during the control task or in any other frequency band.

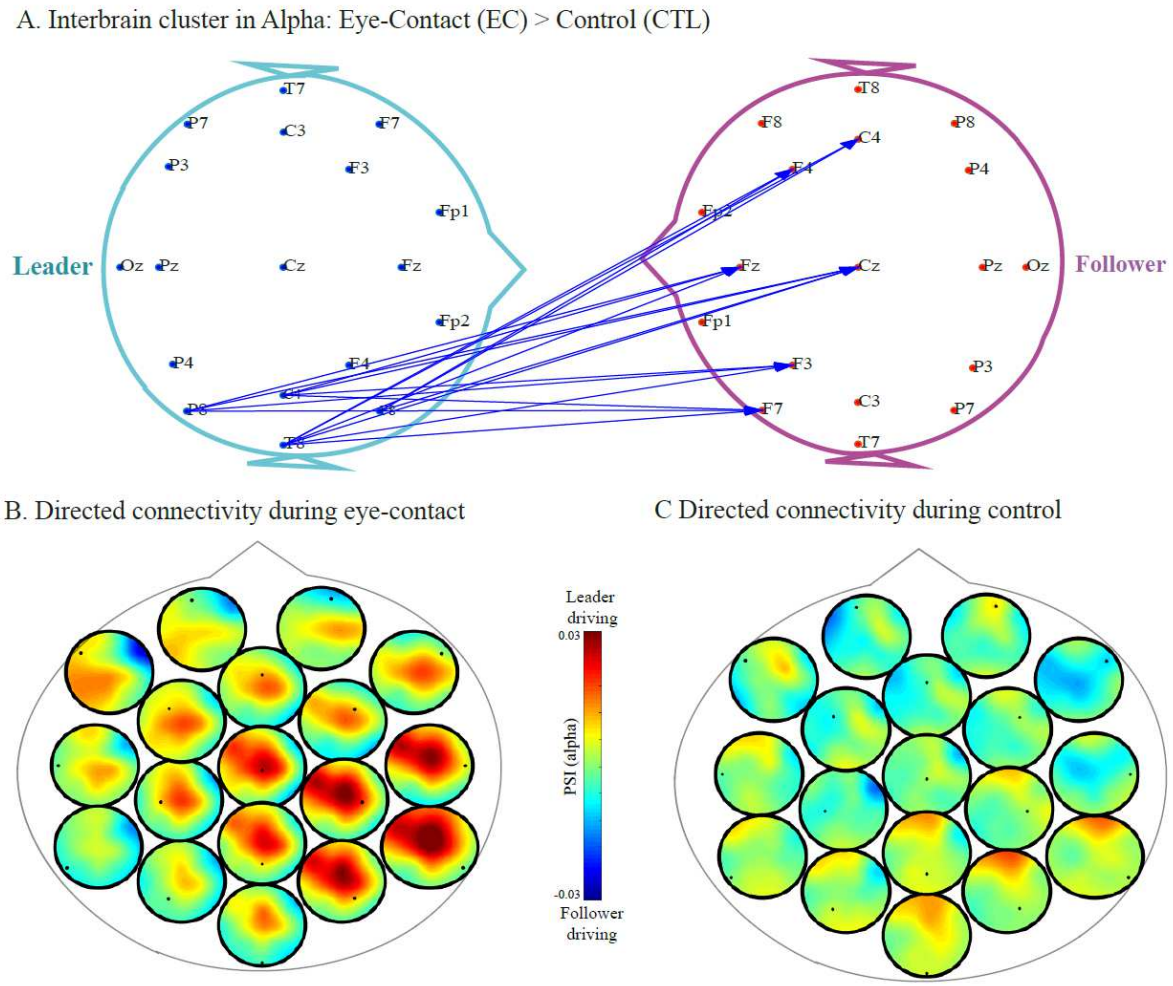

Fig.5. Directed phase synchronization cluster during eye-contact between leaders and followers. **A.** Significant cluster connections from leader (left) to follower (right) in the alpha band. **B.** Heads-in-head representation of the directed connectivity during eye-contact. Each dot represents the channel of the leader in relation to the follower. Red colours mean the channel is driving that area of the follower. For example, the right parietal electrode (P8) seems to be driving the activity of frontal and midfrontal of the follower (represented in red). **C.** The same representation as in B but during the control task.

Intrabrain directed connectivity

We applied nonparametric cluster permutation to the directed intrabrain connections estimated using the phase slope index (PSI) in each frequency band. We followed the same nonparametric cluster permutation approach but taking into consideration the direction of the edges (see Methods). Consistent with the interbrain findings, we observed a significant cluster in the alpha band showing higher synchronization during eye-contact compared to control (*cluster statistic* = 15.737, *t-critical* = 10.157, p = .033), but not in the opposite direction (no cluster for the control > eye-contact task). The cluster shows that during eye-contact, there was higher flux from frontal to parietal and occipital areas (Fig.6A). Fig.6B shows a pattern where posterior regions, especially on the right are driven by frontal and left frontal regions. Clusters in all the other frequency bands were not statistically significant.

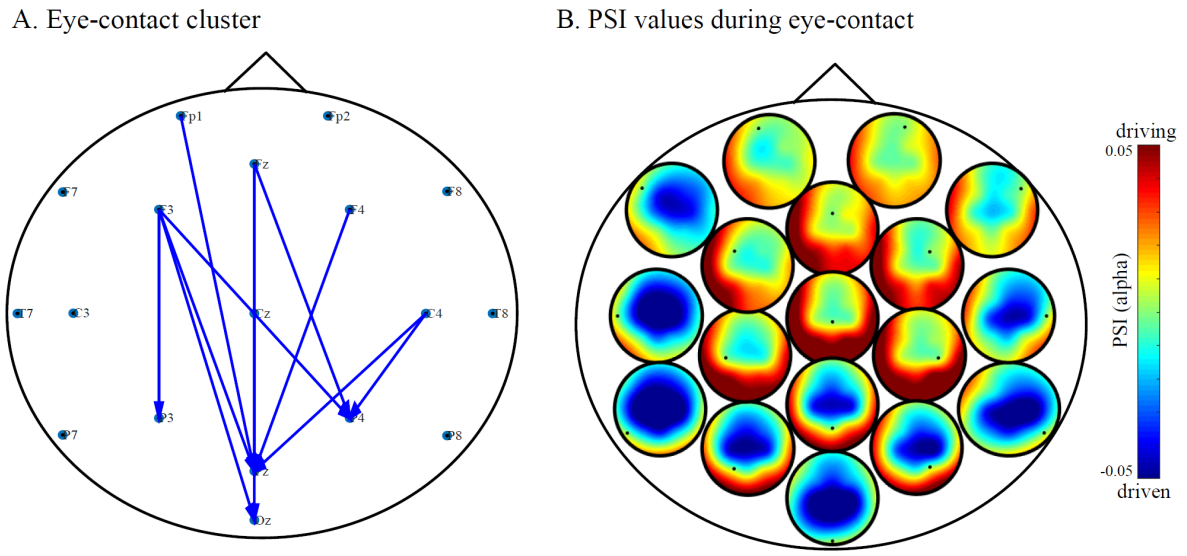

Fig.6. Directed phase synchronization intrabrain clusters during eye-contact. Intrabrain clusters in alpha band. **A.** The arrows show the significant connections for the cluster observed in the alpha band during eye contact compared to the control task. **B.** Heads-in-head plot showing the distribution of the PSI across the scalp for all electrodes. Each sub-topoplot displays how the electrode represented as a dot (labels on A) relates to the rest of the scalp. For example, the central midline electrode (Cz) appears as the "driver" of the alpha phase of the posterior electrodes. Overall, there is a pattern of frontal regions driving posterior areas, which seems to be higher during eye-contact compared to control (A).

Network analysis of the directed networks

We extracted graph theoretical measures for each pair following the same procedures adopted for coherence based on the thresholded matrices. We extracted the same measures as in the previous analysis but now considering the bidirectional matrix (see Methods). To evaluate whether eye-contact was associated with higher changes in intra vs. interbrain edges, we compared the networks average strength and density. The results reported in the supplementary (Fig.S4) demonstrated that eye-contact was associated with higher increase in interbrain connectivity compared to intrabrain during eye-contact, independently of the leadership strength.

Our main hypothesis was that the direction of the synchronization would be from leader to follower. To test this, we counted the proportion of outgoing connections compared to incoming from leaders to followers (Fig.7B). We entered the proportion of outgoing edges (against incoming edges) in a 2 (*leader vs. follower*) x 2 (*leadership strength: strong vs. weak)* between-subjects ANOVA. We observed that the leaders presented a significantly higher proportion of outgoing connections compared to followers ($F(1,94) = 5.642$, $p = .020$, *partial* $\eta^2 = .057$) and a significant interaction with *leadership strength* ($F(1,94) = 13.500$, $p < .001$, *partial* $\eta^2 = .126$) since the leaders showed significantly higher number of outgoing connections compared to followers in strong leadership pairs ($t(40) = 2.946$, $p = .005$), which was not the case for the group with weak leadership ($t(40) = 1.751$, $p = .083$). To investigate the general effects of leadership on interbrain connectivity strength, we compared the strength (z-scores) of outgoing (from leader to follower) vs. incoming (follower to leader) connections using a 2 (leaders vs. followers) x 2 (strong vs. weak leadership) x 2 (outgoing vs. incoming connections) mixed-design ANOVA. We observed a significant three-way interaction ($F(1,94) = 9.010$, $p = .003$, *partial* $\eta^2 = .087$) since there was a significant higher strength of outgoing connections

from leaders compared to followers within pairs with strong leadership ($t(40) = 2.744$, p = .009), but not for the pairs with weak leadership ($t(54) = -.944$, $p = .349$). As predicted, there was no difference between leaders and followers regarding the strength of incoming connections ($p > .3$).

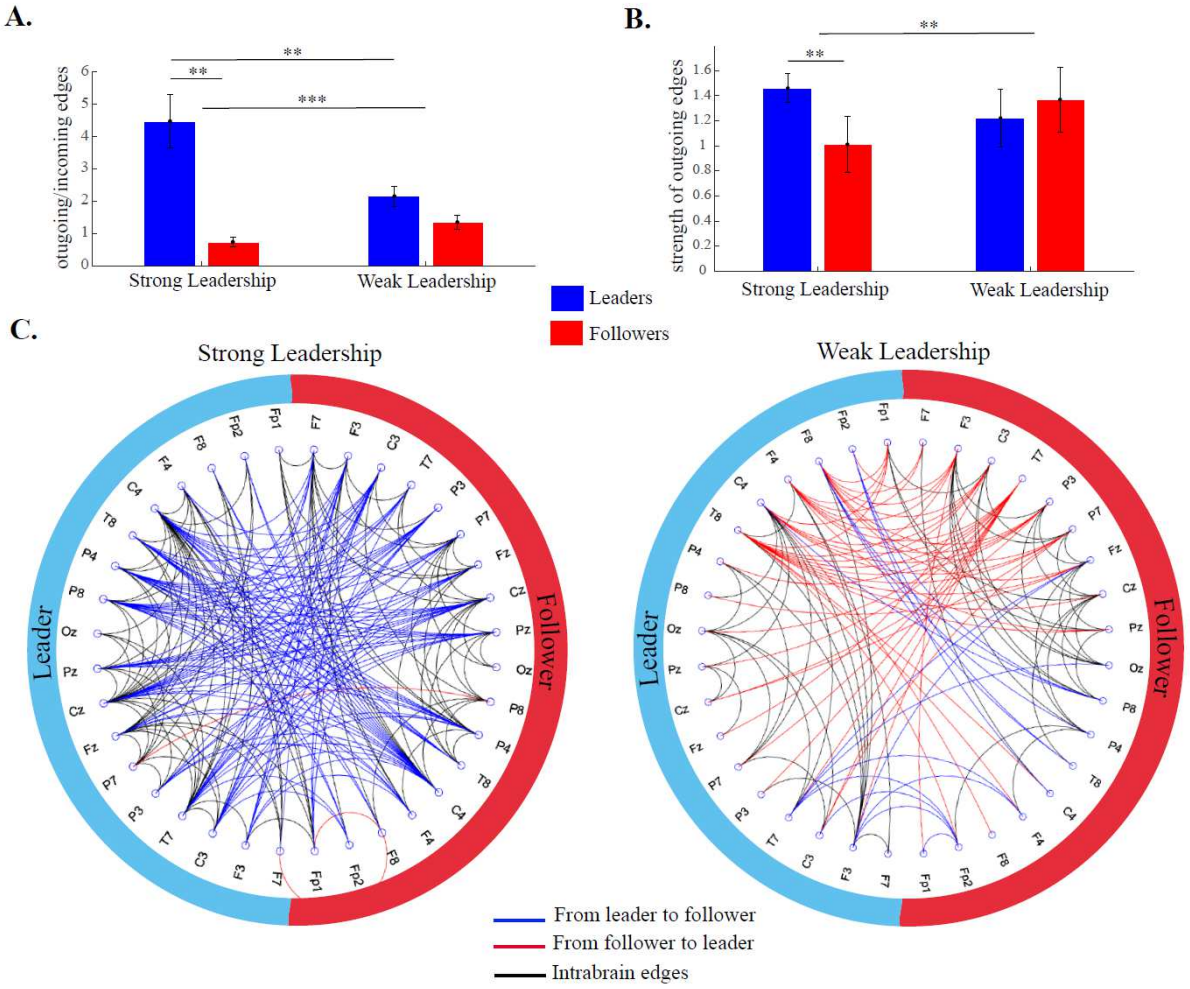

Fig.7. Interbrain connections networks: directed connectivity (PSI) during eye-to-eye. **A.** Proportion of interbrain outgoing in relation to incoming edges in leaders (blue) and followers (red) during eye-contact in pairs with strong and weak leadership strength. **B.** Strength of interbrain outgoing edges in leaders and followers during EC in pairs with strong and weak leadership. **C.** Circular display of the intra and interbrain networks during eye-contact for pairs with strong (left hand side) vs. weak (right hand side) leadership strength. The blue edges represent connections from leader (left) to follower (right); the right edges represent connections from follower to leader; black represents intrabrain edges. These measures are based on the networks thresholded at 1SD against the control task. Error bars represent ±1 SEM. *** $p < .001$/** $p < 0.01$/ * $p < .05$.

We extracted the main network properties of each pair and compared them between pairs with strong vs. weak leadership. For these analyses, 1 pair was excluded because of lack of interbrain connections. We did not observe any statistically significant difference between

pairs with strong vs. weak leadership regarding their networks' global properties, including global efficacy ($t(46) = 1.238$, $p = .222$), average local efficiency ($t(46) = 1.067$, $p = .292$), modularity ($t(46) = .237$, $p = .813$), and assortativity ($t(46) = 1.200$, $p = .236$). Fig.7C illustrates the thresholded average networks of pairs with strong vs. weak leadership.

To investigate which regions in the network are more likely to serve as hubs, we calculated the number of connections (including all incoming and outgoing edges), global and local efficiency per channel, and averaged per ROI. We conducted a 2 (*leadership strength: strong vs. weak*) x 8 (*ROI*: LF, RF, LP, RP, RCT, LCT, MF, MP) x 2 (*who leads: leader vs. follower*) mixed design ANOVA. We observed no significant effect ($p > .1$) except for a marginal trend towards higher degree for participants in pairs with strong leadership ($F(1,92) = 3.121$, $p = .081$, *partial* $\eta^2 = .033$). The results showed that the number of edges was similar across ROIs and for leaders and followers, but slightly higher in participants in strong leadership pairs. To investigate the role of these ROIs in the networks, we extracted the global and local efficiency of each node and averaged across different ROIs. The global efficiency by node represents how much access to the whole network a certain node has. We conducted a 2 (*leadership strength: strong vs. weak*) x 8 (*ROI*: LF, RF, LP, RP, RCT, LCT, MF, MP) x 2 (*role: leader vs. follower*) mixed design ANOVA (Fig.8). We observed no effect for ROIs, leadership and of role. However, there was a marginally significant interaction between *leadership strength* and *role* ($F(1,92) = 4.256$, $p = .042$, *partial* $\eta^2 = .044$) as the leaders of pairs with strong leadership showed higher global efficiency (Fig.8A), especially on the midfrontal and right centro-temporal areas (Fig.8A). We conducted the same analysis using local efficiency as the dependent variable and observed no main effect or interaction between any of the factors ($p > .05$). Altogether these results suggest that the leaders' brains might have more access to the network (mainly through the medial and right posterior regions of the brain) than the follower's brains.

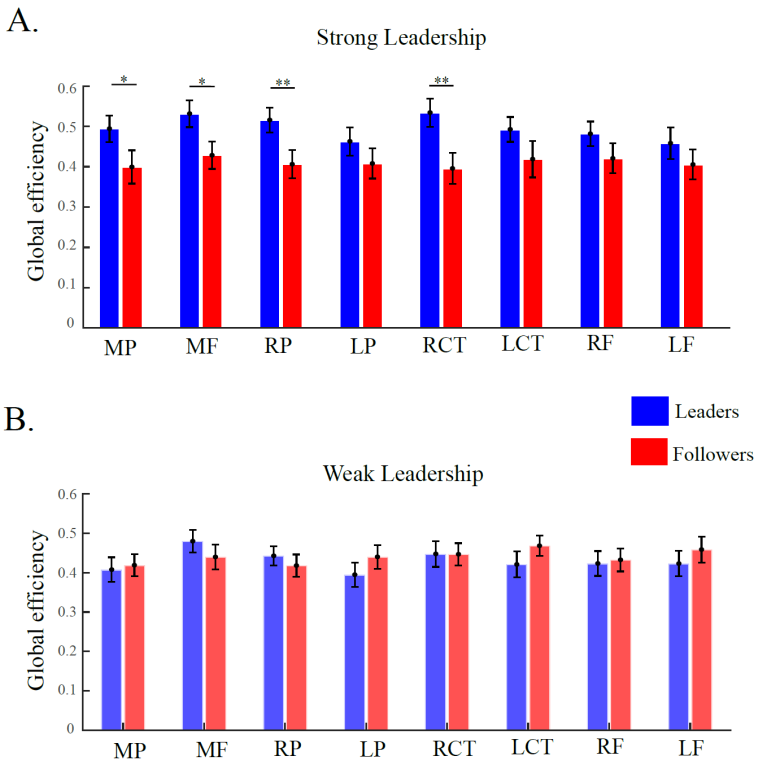

Fig.8. Global efficiency per ROI. **A.** Global efficiency for leaders (blue) and followers (red) per ROI for pairs with strong leadership (darker). **B.** Global efficiency for leaders (blue) and followers (red) per ROI for pairs with weak leadership (lighter). Error bars represent ±1 *SEM*. *** $p < .001$/** $p < 0.01$/ * $p < .05$.

Discussion

This is the first study to investigate how eye-contact affects connectivity from within a brain to the hyperbrain, looking at both directed and undirected synchronization. By combining statistical and graph theoretical methods, we contribute six key findings: 1) eye-contact was associated with higher connectivity between two brains compared to within a single brain, for both undirected and directed connections; 2) eye-contact affects inter and intrabrain synchronization in the same frequency: gamma band for undirected connectivity and alpha band for directed synchronization; 3) the eye-contact hyperbrain network has a rich-club structure with hubs in the midline and right parietal brain areas; 4) friends making eye-contact have stronger interbrain connections; 5) interbrain synchronization flows from leader to follower; 6) the leaders' brain have more access to the entire network than the followers. These findings reveal key insights into the dynamics of eye-contact as discussed below.

Eye-contact involves a network of regions, most consistently those involved in social cognition such as the medial prefrontal cortex (mPFC)[46,47] with the anterior cingulate cortex[48], the superior temporal sulcus and fusiform gyrus[10,49], and the right temporoparietal junction (rTPJ)[50]. Looking into the someone's eyes instead of the mouth was found to increase coupling between rapid and slow routes of visual processing, between the dorsolateral prefrontal cortex (dlPFC) and regions involved in processing intentionality (posterior part of the superior temporal sulcus and medial prefrontal cortex) and within the social brain network[50]. On the other hand, hyperscanning studies using fNIRS observed that eye-contact increases coherence between two brains[12–14] within brains[13]. A two-person neurofeedback study[51] using EEG in a museum setting showed that the amount of eye-contact was positively correlated with

coherence in alpha (9-11Hz) and beta (26-30 Hz) – although gamma (>30Hz) was not tested. No studies on eye-contact have directly compared changes within and between brains' connectivity nor looked at the effects of eye-contact on the wider hyperbrain network. We found clear evidence that eye-contact promotes higher changes in between-brains (interbrain) synchrony compared to within (intrabrain), for both directed and undirected networks. Critically, these increases in connectivity between brains during eye-contact are functionally meaningful, they were higher for friends compared to strangers and they were directed from leaders to followers. These findings support the interactive brain hypothesis[52–54] which posits that examining the brain alone is not sufficient for understanding the kind of synchronization we observe in social interactions. One of the most contentious points of this hypothesis is that the synchronization between brains can be more informative of the nature of the social interaction than the individual brains. We observed that even though the intrabrain connections presented much higher absolute values (due to the physical links and higher intrabrain correlation of EEG signals), the interbrain connections were far more sensitive to eye-contact (i.e. social interaction).

We showed that both within and between brain synchronization associated with eye-contact occurred in the same frequency depending on whether it was undirected (gamma) or directed (alpha) suggesting that intra and interbrain connections are part of the same network. Undirected connectivity was found in the highest frequency band while directed connectivity was observed in a lower frequency band, in line with the proposed functional roles of these frequencies in the brain. There is evidence that top-down attentional processes involve lower frequencies while gamma synchrony reflects bottom-up attention[55]. There is also evidence that lower frequencies enslave or coordinate higher frequencies as demonstrated in cross-frequency coupling studies[56,57]. For instance, alpha was found to modulate neuronal firing (in higher frequencies)[58]; it was also found that high gamma power (80-150Hz) is phase locked to theta oscillations[59]. Regarding the synchronization between brains, the suggestion is that top-down modulations would happen in lower frequencies since they would enslave higher frequencies. Here, our directed connectivity analysis revealed a lower frequency (alpha) than undirected synchronization (gamma) between the pair.

Previous EEG hyperscanning studies revealed increased synchronization during social interactions in a number of different frequencies, most notably in alpha (for a review on EEG hyperscanning studies, see[60]). For instance, Dumas et al. (2010) observed increases in phase synchronization between a model and an imitator in alpha, beta and gamma frequencies. Another study[61] found that effective social coordination was associated with an increase in synchronized alpha in the right centroparietal regions between a pair. Other studies[62–64] observed increased interbrain synchrony in higher frequencies. A difficulty in reconciling these frequency differences is that the activities that the pairs perform vary largely between studies, making it harder to disentangle activity reflecting social coordination and task constraints[15]. In our experiment, we evaluated synchronization during fixations (when both participants eyes were still), which reduces the influence of joint actions/movement on brain synchronization. We suggest that during eye-contact, gamma frequency helps to integrate activity by constantly adjusting to the small movements or changes in the partner's expression since eye-contact leads to synchronized eye movements or mimicking behaviour[48]. This would account for the greater synchrony between friends since it is possible that the frequent exposure helps friends learn each other's patterns of movements which could facilitate mimicry. We also found that leader to follower synchrony occurred in alpha, which is consistent with the physiological interpretation of lower frequencies enslaving higher ones. Although we did not test cross-frequency coupling between the partners, it is possible that the leader's rhythms enslaved the higher frequency eye-contact processes of the follower. Here we suggest that simultaneous

synchronization between participants reflects an increase in synchrony in higher frequencies while directional interactions will be reflected in synchronization in lower frequencies.

We observed that the right parietal and midparietal and midfrontal regions may serve as hubs of the eye-contact network, in both directed and undirected interactions. One of the few studies looking at interbrain synchronization during eye-contact[13] observed an increase in connectivity within and between brains during eye-contact compared to looking at the eyes in a photo of a face. They observed an increased in connectivity between left frontal regions of one participant to left temporoparietal areas of the other, however it is unclear if the increase in interbrain synchronization and its lateralization were associated with the difference between gazing at a live face vs. a still photo as it has been demonstrated that live mutual eye-contact involves different neural mechanisms than those involved in delayed off-line eye-contact[48]. For instance, eye-contact has been shown to be associated with increased activity in the rTPJ compared to looking at a video of a dynamic face[14]. An increase in interbrain rTPJ coupling was also found by a study[12] looking at eye-contact during live interactions. While we cannot know the precise neural sources of this effect due to our limited spatial resolution, we can generate predictions regarding the dynamics of the interactions based roughly on the locations of these areas on the scalp and the previous literature on eye-contact and social interactions. An insightful review[65] pointed out that hyperscanning studies often find that multiple brain regions synchronize during social interactions. They suggested that it is important to investigate the extent to which interbrain dynamics vary across different regions. We provide evidence that some regions might play a key role in the eye-contact network by integrating external and internal online information about the self and their eye-contact partner. The midline regions we observed might reflect the activity of the medial prefrontal cortex and the posterior cingulate cortex, both along the midline. The mPFC and the PCC were both found to be involved in mentalizing[66,67]. The mPFC was found to control the level of mimicry driven by eye-contact by modulating sensory processes in the superior temporal sulcus (STS)[47]. There is evidence that while regions of the mPFC and ventromedial PFC are biased for self-referential processing, the PCC and/or the precuneus, and the right temporoparietal junction are biased for other-referential processing[68–71]. Here we suggest that these areas, the medial frontal, medial posterior and the right parietal may serve as hubs which integrate information about the self (internal connections) and the other (represented as the interbrain connections) during eye-contact, enabling interbrain synchronization.

Finally, we observed that effective connectivity flux went from leaders to followers. Previous studies have observed similar leader-follower directed connectivity during music playing[35,72] and group discussions[33]. It has also been observed[34] that during a leader-follower finger tapping task, the leader showed stronger frontal alpha desynchronization than the follower. Building on this idea, a computational modelling study demonstrated that in leader-follower interactions, the leader shows the highest within-unit coupling (in our case intrabrain) and the follower the lowest within unit coupling[37]. We did not find evidence of differential intrabrain coupling between leader and follower in our study, which might be because our paradigm did not require mutual and continuous adaptation between leader and follower. Instead, we found that the leaders' brain regions had more access to the entire network of leader-follower (i.e. hyperbrain). This means that the nodes of the leader's brains have shortest paths through the entire network, increasing its accessibility. Future studies could investigate how this can affect the amount of control that the leader's brain exerts in the dyad's behaviour in mutually interactive tasks.

Methods

Participants

Fifty-six pairs of participants (112 participants in total) took part in this experiment, all neurologically healthy adults. Of those, 27 pairs were friends (37 female, 17 male) with a mean age of 20.52 (*SD* = 1.59) years, while 29 were strangers (45 female, 13 male) with a mean age of 20.30 (*SD* = 2.30) years. All participants received a monetary compensation of £7.50 per hour for their participation and gave written informed consent before the beginning of the experiment. Participation was voluntary and the participants were reminded that they could withdraw at any point without any consequence. The study protocol was approved by the local ethics committee at Queen Mary University of London. Experiments were conducted in accordance with the World Declaration of Helsinki (1964).

Procedure

Participants arrived in pairs and sat opposite one another in a quiet lab room. First, the experimenters prepared the EEG equipment on both participants, so that each was connected to an EEG machine (Fig.1A). Subsequently, an eye tracker was positioned eye-level in front of each participant, so that each machine captured their respective eye movements. Each participant used a chinrest that was at the same height for both partners. For the eye-trackers to register the position and movement of the eyes, the eye tracking machines were calibrated with the following procedure. To calibrate the eye-tracking of participant on seat 1 (P1), the participant on the opposite seat (P2) held a calibration board with numbers 1-9 written on a 3 * 3 grid. P1 was instructed to look at each number for 5 seconds, while the positions of their eyes were registered on the computer and then the same was repeated for P2. Participants' eye movements were recorded at 60 Hz resolution. Earphones were provided and the sound volume was adjusted at a comfortable level. In all tasks, participants were presented with 1000-Hz tones which were either 'short' (1.5 sec) or 'long' (2.5 secs) in duration. There were 4 conditions that were presented randomly across trials 1) P1 and P2 both heard a short tone; 2) P1 and P2 both heard a long tone; 3) P1 heard a short and P2 a long tone; and 4) P1 heard a long and P2 a short tone. The order of the tasks (eye contact and control) was counterbalanced across pairs.

Eye-contact task (EC)

Participants were instructed to fixate on a black sticker positioned on the chin rest of their partner. They were then required to pay attention to the duration of the beep that would be presented to them through the earphones. When the beep ended, they were required to look at their partner's eyes for the duration of the beep they had just heard (they were asked to try to estimate the duration of the beep and reproduce the same duration). To indicate the end of their estimation, they looked back at the sticker until the next trial (Fig.1B). The first 45 pairs were presented with 56 trials in total (14 trials in each of the four conditions: short-short, long-long, short-long, long-short tones), while the number of trials was doubled for the last 11 pairs to increase statistical power (112 trials in total).

Control task (CTL)

To compare brain synchrony during eye-contact vs. no eye-contact, we conducted a control task where participants were required to look at their partner's eyes when the latter was looking at the chinrest, and vice versa (Fig.1C). For instance, P1 was required to fixate on P2's eyes until the tone was presented. After the tone finished, P1 looked at P2's chinrest-sticker for the duration of the beep and returned to looking at the eyes once they had finished reproducing the duration. The other participant was instructed to do the opposite, first gaze down while listening to the beep and then reproduce the tone duration by staring at their partner's eyes.

Therefore, in these control trials, the pair never made eye contact. The condition was repeated reversing the roles. Pairs were presented with 28 trials in each of these two control blocks, 56 trials in total. The number of trials was doubled for the last 11 pairs. Trials were randomized across conditions. The order of the EC and CTL tasks was counterbalanced across pairs.

EEG recording and preprocessing

The EEG signals were recorded using two Starstim 20 (Neuroelectrices) EEG devices. We used eighteen PiStim electrodes placed according to the extended 10-20 electrode placement system (Jasper, 1958). The EEG electrodes were: P8, F8, F4, C4, T8, P4, Fp2, Fp1, Fz, Cz, Pz, Oz, P3, F3, F7, C3, T7, and P7. After data collection, the EEG data were re-referenced to the algebraic mean of the right and left earlobe electrodes[73]. Continuous data were high-pass filtered at .5 Hz and low-pass filtered at 45 Hz. Data from electrodes with poor signal quality, as observed by visual inspection, was interpolated from neighbouring electrodes. The data was epoched according to the onset of the common tone-reproduction period. Specifically, the start of the epoch corresponded to the time when both participants started reproducing the tone duration. The offset of the epoch corresponded to the time when one of the participants finished reproducing the tone. Independent component analysis could distort the phase of the signal which would in turn affect connectivity. We thus detected eye blinks automatically by identifying the time points of the signal when Fp1 and Fp2 electrodes had amplitude exceeding +/-70 μV, and excluded +/-0.040 sec from the data of all electrodes from subsequent analysis. The preprocessing was done using EEGLAB toolbox[74]. One pair was excluded from the EEG analysis due to technical issues in the EEG recording, while five more pairs were excluded due to insufficient number of valid trials (<5 trials per condition) ascribed to motor artefacts (N = 100, 50 pairs).

Data analysis

Tone-reproduction duration

We compared participants' gaze durations during tone duration reproduction. Specifically, we calculated the mean tone-reproduction duration of each participant (i.e. offset minus onset of eye movement during reproduction of the tone duration), separately in each task and in each condition. As we wanted to investigate whether the tone-reproduction duration of one participant would be influenced by their partner, a 2 *(task: EC vs. CTL)* x 2 *(tone duration: short vs. long)* x 2 *(pair duration: same vs. different)* repeated measures ANOVA was conducted. We note here that *same pair duration* corresponds to the trials when both partners heard a short or a long tone, whereas *different pair duration* corresponds to trials when one partner heard a short tone and the other partner heard a long tone. Gaze durations of <0.5 or >4 secs were excluded.

Evidence for interaction between partners

In order to test whether the partners were truly interacting during the eye-contact condition (EC), we tested the correlation between their tone-reproduction durations. If the behaviour of one participant affected their partner, we would expect that they would make similar duration estimates when presented with tones of the same duration. We only used trials when both partners were presented with short or long tones, in order to avoid inflating the correlations due to different tone durations. Pairs with less than 5 trials were excluded from the analysis. We expected that if the participants were truly interacting: 1) the time estimations of short and long intervals would change if their partner heard to a different duration; 2) the

partners' time estimations would be correlated (Spearman correlation within trials) compared to the shuffled distribution of the same trials; 3) these effects would be stronger in the eye-contact condition.

First, for each pair, we tested the correlation between their tone-reproduction durations on trials where both participants heard the same duration in each condition (EC vs. CTL). Second, since there was still a small degree of interaction in CTL (participants might have been able to see their partner's behaviour), we compared the correlation between the intervals against a shuffled distribution. For each participant, we shuffled the order of the trials (we did not shuffle between participants), and tested the correlations between partners for 5000 iterations. We then extracted the mean and standard deviations of the random distribution for each pair. Finally, we investigated whether their actual correlation value was higher from chance level as follows by statistically comparing the correlations obtained from the real data with the average correlations from the randomly shuffled data.

Non-directed brain synchronization during eye-contact

Coherence: To compare brain synchronization between the EEG signals of the partners during eye-contact vs. control (no eye-contact), we calculated coherence, a non-directed measure of functional connectivity. Coherence represents the consistency of the phase difference between two signals at a given frequency. It is computed by normalizing the magnitude of the summed cross-spectral density between two signals by their respective power. The coherence values range between 0 (low) and 1 (high). We first conducted a Fourier analysis in steps of 0.67 Hz on the following frequency bands: theta (4-7 Hz), alpha (8-12 Hz), lower beta (13-20 Hz), upper beta (21-30 Hz), and gamma (30-45 Hz). Coherence was calculated in the analyzed frequency bands. As the EEG data immediately after eye movement were noisy, we analyzed the time window 0.5-2 sec after the onset of each epoch. Trials with shorter durations were excluded from the EEG analysis.

Brain synchronization during eye-contact vs. control task

Nonparametric cluster permutation test. As there was no solid assumption to justify a hypothesis-driven analysis and considering the multiple comparisons problem, we used nonparametric cluster permutation approach[75] to compare the synchronization of oscillatory activity during eye contact (EC) vs. control task (CTL). To eliminate potential biases introduced by multiple comparisons and distribution assumptions of parametric tests, the difference distribution for EC vs CTL networks was constructed in a data-driven manner using label randomizations combined with a network-based clustering criterion for the *t*-statistic extraction[76]. The network-based statistic (NBS) controls for family-wise error rate offering a substantial gain in power by considering the topological characteristics of the graph assuming that a biologically relevant effect on the network cannot be isolated to single or disconnected edges. Meaningful clusters need to show strongly connected components (connected to each other). In this study, we first calculated the statistical difference for each brain edge (EC vs. CTL), discarding absolute *t*-values lower than 2. Then, the survived edges were clustered in strong connected components (SCCs; partition into subgraphs with the property of having at least one path between all pairs of nodes) depending on whether they reflect identical effects (separate clusters for positive and negative edges). Subsequently, difference distribution curves of the condition differences were estimated using 5000 permutations by randomly shuffling the condition labels, respecting each pair's (for interbrain tests) or each participant's (for intrabrain

tests) data. In each iteration, we computed the sum of *t*-scores within each cluster and kept the maximum (absolute value) cluster score as the cluster *t*-statistic. The *t*-critical values were then calculated to align with the significance level of .05 (two-tailed). Clusters formed by the actual labels with t-score exceeding the *t*-critical values were finally identified following an SCC-wise inference on the difference distribution. This approach was used in all cluster analyses presented in this paper, both intra and interbrain.

Effect of leadership on directed brain synchronization

To investigate how interbrain synchronization is influenced by leadership roles, we first identified the leader and the follower in each pair. Then, we compared directed brain synchronization in pairs with strong vs. weak leadership patterns. Therefore, in each trial, the person who broke eye-contact from their partner first was considered the leader. We divided the number of trials in which participant 1 (P1) broke eye contact first compared to the total number of trials. The resulted values spanned from 0 (P2 leads) to 1 (P1 leads). Values around 0.5 meant the absence of a leader (P1 and P2 broke eye-contact in an approximately equal number of trials). As values around both extremes are indicative of strong leadership (e.g., 0.2 signifies the same leadership strength as 0.8; in the first case P2 is the leader, whereas in the second case P1 is the leader), we subtracted all values that were lower than 0.5 from 1. This resulted in values ranging from 0.5 to 1, with higher values indicating stronger leadership pattern. We used trials when both participants heard tones with the same duration (both short or both long).

We then split the pairs into two groups based on their leadership strength (median split) and found that only one pair displayed no leadership relationship between partners. This pair was excluded from this analysis, leaving 49 pairs in total. Pairs with strong leadership relationship (higher than the median leadership strength at 0.667) were considered as the *high leadership group* (HL; N = 26), whereas pairs with weak leadership relationship were considered the *low leadership group* (LL; N = 23).

Phase slope index (PSI). Directed interbrain synchronization was measured using the phase slope index (PSI)[77] to estimate the synchronization between the electrodes of leaders and followers. If PSI from electrode X (leader) to electrode Y (follower) is positive this would mean that the leader is 'leading' the brain synchronization. The PSI estimates the synchronization between two signals based on the slope of the phase of their cross-spectrum, and is insensitive to volume conduction while detecting non-instantaneous functional relations between two signals. In Nolte et al. (2008), PSI is defined as:

$$\tilde{\Psi}_{ij} = \Im\left(\sum_{f\in F} C_{ij}^{*}(f)C_{ij}(f+\delta f)\right) \quad (1)$$

where:

$$C_{ij}(f) = \frac{S_{ij}(f)}{\sqrt{S_{ii}(f)S_{jj}(f)}} \quad (2)$$

is the complex coherency between sources i and j, S is the cross-spectral matrix, δf is the frequency resolution of the coherency, and $\Im(\cdot)$ denotes getting the imaginary part. F is the set of frequencies over which the slope is summed. The equation is rewritten as follows to see that the definition of $\widetilde{\Psi}_{ij}$ corresponds to a meaningful estimate:

$$\widetilde{\Psi}_{ij} = \sum_{f \in F} a_{ij}(f) a_{ij}(f + \delta f) \sin\big(\Phi(f + \delta f) - \Phi(f)\big) \tag{3}$$

with $a_{ij}(f) = \big|C_{ij}(f)\big|$ being frequency dependent weights. For smooth phase spectra, $\sin\left(\Phi(f + \delta f) - \Phi(f)\right) \approx \Phi(f + \delta f) - \Phi(f)$ and hence Ψ corresponds to a weighted average of the slope.

Finally, $\widetilde{\Psi}$ is normalized by an estimate of its standard deviation:

$$\Psi = \frac{\widetilde{\Psi}}{std\big(\widetilde{\Psi}\big)} \tag{4}$$

with $std\big(\widetilde{\Psi}\big)$ being estimated by the Jackknife method.

Nonparametric cluster permutation on PSI networks: we employed the same approach described above. However, since the PSI is directed, we calculated the clusters (SCCs) separately considering whether the connections were positive or negative and whether they were higher during eye-contact or control. This avoided mixing up connections that belonged to different effects.

Coherence thresholding for hyperbrain analyses

For each pair k of participants with a sufficient number (>5) of trials in both the EC and CTL tasks, we computed the Z-scores for the coherence measured between the electrodes' signals. For each possible intrabrain or interbrain edge (i, j), the coherence Z-score at a given frequency band f was computed as:

$$Z_{i,j}^{k}(f) = \frac{C_{i,j}^{k}(f) - \mu_{i,j}^{k}(f)}{\sigma_{i,j}^{k}(f)}, \tag{5}$$

where the mean value $\mu_{i,j}^{k}(f)$ and the standard deviation $\sigma_{i,j}^{k}(f)$ were computed individually across all the edges (i, j), during the CTL for the k couple (for interbrain edges, i indexes P1 nodes and j indexes P2 nodes).

Since we noticed higher coherence values in intrabrain vs. interbrain connections, we adopted two separate thresholds for the two types of edges, whereas for the intrabrain edges, Z-scores were calculated in the single-subject level to balance between the count of intrabrain connections within a particular pair.

Hyperbrain networks from Z-scores

Single-pair Z-transformed connectivity matrices were further processed to generate both an unweighted and a weighed graph representation. Using both the Z-thresholds of P1 and P2, we obtained *(i)* an unweighted graph from each single-pair connectivity matrix by

binarizing the z-scores above and below the Z-threshold of 1 and *(ii)* a weighted graph version of the same data simply by ditching the below-threshold connections.

Graph theoretical measures

Efficiency quantifies the extent to which a network is structurally efficient in exchanging information using shortest paths. To this end, the efficiency between any pair of nodes (i, j) is defined as being inversely proportional to their shortest distance $d_{i,j}$ on the network.

- *Global Efficiency (E)* of an unweighted network $\boldsymbol{G}$ with N nodes is defined as the average efficiency in the communication between pairs of nodes, where the average is evaluated over all the couples of nodes $(i, j) \in \boldsymbol{G}$,[78]:

$$E(\boldsymbol{G}) = \frac{1}{N(N-1)} \sum_{i \neq j} \frac{1}{d_{i,j}} \tag{6}$$

- *Local Efficiency (E_{loc})* characterizes the local properties of a graph $\boldsymbol{G}$. It is obtained by evaluating the efficiency of each local subgraph $\boldsymbol{G_i}$ for each of the $i = 1, \dots, N$ nodes of the whole graph. Given a node i, the subrgraph $\boldsymbol{G_i}$ is constructed by considering the subgraph induced by node i and its k_i first neighbors and by removing node i from this subgraph. Hence, the local efficiency of the network is defined as the average across all the subgraph $\boldsymbol{G_i}$ efficiencies:

$$E_{loc}(\boldsymbol{G}) = \frac{1}{N} \sum_{i \in \boldsymbol{G}} E(\boldsymbol{G_i}) \tag{7}$$

Community is a subset of the graph nodes such that the nodes belonging to the same community areon average more connected than the nodes belonging to different communities. We call *community partition* a representation of the graph as non-overlapping communities[79].

Modularity measures the difference between the fraction of links connecting nodes belonging to the same community in the actual graph and its expected value in a random graph[80]. Hence, the higher is the modularity the more significant is the community partition. For the hyperbrain networks, a natural community partition is defined by separating the nodes in two communities, namely the nodes of P1 (leader) and P2 (follower). In the case of directed weighted graphs with weights $w_{i,j}$, modularity is defined as[80]:

$$Q = \frac{1}{W} \sum_{i,j} \left(w_{i,j} - \frac{s_i^{out} \cdot s_j^{in}}{W} \right) \cdot \delta(C_i, C_j), \tag{8}$$

where $W = \sum_{i,j} w_{i,j}$ (sum of weights), $s_i^{out} = \sum_j a_{i,j} w_{i,j}$ (sum of outward weights), $s_j^{in} = \sum_i a_{i,j} w_{i,j}$ (sum of inward weights), $a_{i,j}$ denotes the (i, j) adjacent matrix elements (binary) and $\delta(C_i, C_j)$ is equal to 1 if i and j belong to the same set of nodes (P1 or P2), and is 0 otherwise.

Assortativity measures the tendency of the nodes in a network to be connected to other nodes following similar patterns. In general, if a population of nodes can be divided in different

discrete types of nodesaccording to some countable nodes characteristic, the assortativity coefficient r is defined as[81]:

$$r = \frac{\sum_i e_{ii} - \sum_i a_i b_i}{1 - \sum_i a_i b_i}, \tag{9}$$

where $e_{ij}$is the fraction of edges from nodes of type i to nodes of type j (i.e. $\sum_{ij} e_{ij} = 1$), $a_i = \sum_j e_{ij}$ and $b_i = \sum_j e_{ji}$. The assortativity coefficient ranges from -1 to 1. For $r = 1$ we have perfect assortativity, for $r = 0$ the network is non-assortative, while for $-1 \leq r < 0$ we have perfect disassortativity. In particular, we focused on the assortativity of degree, i.e. when i and j are the node degrees.

Rich-club coefficient: The *rich-club phenomenon* in a network describes the tendency of the nodes with a large number of edges (the hubs or *rich nodes*) to be well-connected to each other, forming tightly interconnected subgraphs (*clubs*)[82,83]. It can be quantified by computing the so-called *rich-club coefficient* as a function of the degree k as:

$$\varphi(k) = \frac{2E_{>k}}{N_{>k}(N_{>k} - 1)}, \tag{10}$$

where $N_{>k}$ is the number of nodes in the graph **G** with degree greater than k and $E_{>k}$ is the number of edges connecting pairs of nodes having degree larger than k (i.e. $\varphi(k)$ is the fraction of such edges actually present in the network, versus the maximum possible number).

Normalized Rich-club coefficient: Since nodes with high degrees have a high number of incident edges, they naturally tend to be more densely connected than small degree ones. This effect can be taken into account by defining a normalized version of the rich-club coefficient. As a normalization factor we use the rich-club coefficient $\varphi_{ran}(k)$ computed for the maximal random network obtained through two ends swapping of two edges selected uniformly at random in the original network. Hence, the normalized rich-club coefficient is defined as[83]:

$$\rho_{ran}(k) = \frac{\varphi(k)}{\varphi_{ran}(k)}. \tag{11}$$

If $\rho_{ran}(k) > 1$ for large values of *k*, then starting from a certain *k*, a rich-club phenomenon is present in the network.

Authors Contributions:

CDBL: formulated the research question, contributed to the study design, programmed and coordinated data collection, contributed to the analytic ideas, analysed the data, wrote the paper.
IZ: contributed to the study design, supervised and coordinated data collection, preprocessed the neuroimaging data, contributed to data analysis scripts, contributed to writing the paper.
AG: contributed to data analysis both conceptually and on producing the analysis scripts, contributed to writing the paper.
GDB: contributed to data analysis, conducted graph theoretical analysis of the data.
NB: developed the eye-tracking paradigm (with IM), contributed in the design of the study; programmed the initial eye-tracking task (modified by CDBL), contributed to writing and editing the paper.
AC: contributed to data analysis, conducted graph theoretical analysis of the data.
VL: guided the network analysis, contributed to writing and editing the paper.
IM: developed the eye-tracking paradigm (with NB), contributed to the study design and methodological approach, contributed to writing and editing the paper.

Acknowledgments

This research was funded by BIAL Foundation (No. 138/18). V.L. acknowledges support from the Leverhulme Trust Research Fellowship 278 "CREATE: the network components of creativity and success". We would like to thank Tatiana Adamczewska for her drawing of the paradigm (Fig.1) and her contribution to data collection. We would like to thank Dr Frederike Beyer for assistance in setting up the study. We would like to thank the students who contributed to data collection in this project, including: Laelle Disu, Lovejot Kaur, and Angeliki Plessa.

References

1. Bard, K. A. *et al.* Group differences in the mutual gaze of chimpanzees (Pan troglodytes). *Developmental Psychology* **41**, 616 (2005).
2. Mulholland, M. M. *et al.* Differences in the mutual eye gaze of bonobos (Pan paniscus) and chimpanzees (Pan troglodytes). *Journal of Comparative Psychology* **134**, 318 (2020).
3. Kobayashi, H. & Kohshima, S. Unique morphology of the human eye. *Nature* **387**, 767–768 (1997).
4. Sato, T. Effects of viewing distance and image resolution on gaze perception. *Human Interface Society* **2**, 127–131 (2000).
5. Emery, N. J. The eyes have it: the neuroethology, function and evolution of social gaze. *Neuroscience & biobehavioral reviews* **24**, 581–604 (2000).
6. Adolphs, R. The social brain: neural basis of social knowledge. *Annual review of psychology* **60**, 693–716 (2009).
7. Senju, A. & Johnson, M. H. The eye contact effect: mechanisms and development. *Trends in Cognitive Sciences* **13**, 127–134 (2009).
8. Hoffman, E. A. & Haxby, J. V. Distinct representations of eye gaze and identity in the distributed human neural system for face perception. *Nature neuroscience* **3**, 80–84 (2000).
9. Kampe, K. K., Frith, C. D. & Frith, U. "Hey John": signals conveying communicative intention toward the self activate brain regions associated with "mentalizing," regardless of modality. *Journal of Neuroscience* **23**, 5258–5263 (2003).
10. Pelphrey, K. A., Viola, R. J. & McCarthy, G. When strangers pass: processing of mutual and averted social gaze in the superior temporal sulcus. *Psychological science* **15**, 598–603 (2004).
11. Frith, C. D. & Frith, U. The Neural Basis of Mentalizing. *Neuron* **50**, 531–534 (2006).
12. Dravida, S., Noah, J. A., Zhang, X. & Hirsch, J. Joint attention during live person-to-person contact activates rTPJ, including a sub-component associated with spontaneous eye-to-eye contact. *Frontiers in Human Neuroscience* **14**, 201 (2020).

13. Hirsch, J., Zhang, X., Noah, J. A. & Ono, Y. Frontal temporal and parietal systems synchronize within and across brains during live eye-to-eye contact. *Neuroimage* **157**, 314–330 (2017).
14. Noah, J. A. *et al.* Real-time eye-to-eye contact is associated with cross-brain neural coupling in angular gyrus. *Frontiers in human neuroscience* **14**, 19 (2020).
15. Hamilton, A. F. de C. Hyperscanning: Beyond the Hype. *Neuron* **109**, 404–407 (2021).
16. Hari, R., Henriksson, L., Malinen, S. & Parkkonen, L. Centrality of social interaction in human brain function. *Neuron* **88**, 181–193 (2015).
17. Wheatley, T., Boncz, A., Toni, I. & Stolk, A. Beyond the isolated brain: the promise and challenge of interacting minds. *Neuron* **103**, 186–188 (2019).
18. Anders, S., Heinzle, J., Weiskopf, N., Ethofer, T. & Haynes, J.-D. Flow of affective information between communicating brains. *Neuroimage* **54**, 439–446 (2011).
19. Dikker, S. *et al.* Brain-to-brain synchrony tracks real-world dynamic group interactions in the classroom. *Current Biology* **27**, 1375–1380 (2017).
20. Hu, Y., Hu, Y., Li, X., Pan, Y. & Cheng, X. Brain-to-brain synchronization across two persons predicts mutual prosociality. *Social cognitive and affective neuroscience* **12**, 1835–1844 (2017).
21. Jiang, J. *et al.* Neural synchronization during face-to-face communication. *Journal of Neuroscience* **32**, 16064–16069 (2012).
22. Pan, Y., Novembre, G., Song, B., Li, X. & Hu, Y. Interpersonal synchronization of inferior frontal cortices tracks social interactive learning of a song. *Neuroimage* **183**, 280–290 (2018).
23. Pan, Y. *et al.* Instructor-learner brain coupling discriminates between instructional approaches and predicts learning. *Neuroimage* **211**, 116657 (2020).
24. Reindl, V., Gerloff, C., Scharke, W. & Konrad, K. Brain-to-brain synchrony in parent-child dyads and the relationship with emotion regulation revealed by fNIRS-based hyperscanning. *NeuroImage* **178**, 493–502 (2018).
25. Santamaria, L. *et al.* Emotional valence modulates the topology of the parent-infant inter-brain network. *NeuroImage* **207**, 116341 (2020).

26. Schippers, M. B., Roebroeck, A., Renken, R., Nanetti, L. & Keysers, C. Mapping the information flow from one brain to another during gestural communication. *Proceedings of the National Academy of Sciences* **107**, 9388–9393 (2010).
27. Stephens, G. J., Silbert, L. J. & Hasson, U. Speaker–listener neural coupling underlies successful communication. *Proc Natl Acad Sci USA* **107**, 14425 (2010).
28. Xue, H., Lu, K. & Hao, N. Cooperation makes two less-creative individuals turn into a highly-creative pair. *NeuroImage* **172**, 527–537 (2018).
29. Zhang, Y., Meng, T., Hou, Y., Pan, Y. & Hu, Y. Interpersonal brain synchronization associated with working alliance during psychological counseling. *Psychiatry Research: Neuroimaging* **282**, 103–109 (2018).
30. Yang, J., Zhang, H., Ni, J., De Dreu, C. K. & Ma, Y. Within-group synchronization in the prefrontal cortex associates with intergroup conflict. *Nature Neuroscience* 1–7 (2020).
31. Xie, H. *et al.* Finding the neural correlates of collaboration using a three-person fMRI hyperscanning paradigm. *Proceedings of the National Academy of Sciences* **117**, 23066–23072 (2020).
32. Pan, Y., Cheng, X., Zhang, Z., Li, X. & Hu, Y. Cooperation in lovers: An fNIRS-based hyperscanning study. *Human Brain Mapping* **38**, 831–841 (2017).
33. Jiang, J. *et al.* Leader emergence through interpersonal neural synchronization. *Proceedings of the National Academy of Sciences* **112**, 4274–4279 (2015).
34. Konvalinka, I. *et al.* Frontal alpha oscillations distinguish leaders from followers: multivariate decoding of mutually interacting brains. *NeuroImage* **94**, 79–88 (2014).
35. Sänger, J., Müller, V. & Lindenberger, U. Directionality in hyperbrain networks discriminates between leaders and followers in guitar duets. *Frontiers in human neuroscience* **7**, 234 (2013).
36. Kingsbury, L. *et al.* Correlated Neural Activity and Encoding of Behavior across Brains of Socially Interacting Animals. *Cell* **178**, 429-446.e16 (2019).

37. Heggli, O. A., Cabral, J., Konvalinka, I., Vuust, P. & Kringelbach, M. L. A Kuramoto model of self-other integration across interpersonal synchronization strategies. *PLoS computational biology* **15**, e1007422 (2019).
38. Bullmore, E. & Sporns, O. Complex brain networks: graph theoretical analysis of structural and functional systems. *Nature reviews neuroscience* **10**, 186–198 (2009).
39. Astolfi, L. *et al.* Raising the bar: Can dual scanning improve our understanding of joint action? *NeuroImage* **216**, 116813 (2020).
40. Ciaramidaro, A. *et al.* Multiple-Brain Connectivity During Third Party Punishment: an EEG Hyperscanning Study. *Scientific Reports* **8**, 6822 (2018).
41. De Vico Fallani, F. *et al.* Defecting or Not Defecting: How to "Read" Human Behavior during Cooperative Games by EEG Measurements. *PLOS ONE* **5**, e14187 (2010).
42. Rogers, S. L., Speelman, C. P., Guidetti, O. & Longmuir, M. Using dual eye tracking to uncover personal gaze patterns during social interaction. *Scientific reports* **8**, 1–9 (2018).
43. Binetti, N., Harrison, C., Coutrot, A., Johnston, A. & Mareschal, I. Pupil dilation as an index of preferred mutual gaze duration. *Royal Society Open Science* **3**, 160086 (2016).
44. Shepherd, S. V., Deaner, R. O. & Platt, M. L. Social status gates social attention in monkeys. *Current biology* **16**, R119–R120 (2006).
45. Liuzza, M. T. *et al.* Follow my eyes: the gaze of politicians reflexively captures the gaze of ingroup voters. *PloS one* **6**, e25117 (2011).
46. Calder, A. J. *et al.* Reading the mind from eye gaze. *Neuropsychologia* **40**, 1129–1138 (2002).
47. Wang, Y., Ramsey, R. & de C. Hamilton, A. F. The Control of Mimicry by Eye Contact Is Mediated by Medial Prefrontal Cortex. *J. Neurosci.* **31**, 12001 (2011).
48. Koike, T., Sumiya, M., Nakagawa, E., Okazaki, S. & Sadato, N. What makes eye contact special? Neural substrates of on-line mutual eye-gaze: a hyperscanning fMRI study. *eNeuro* ENEURO.0284-18.2019 (2019) doi:10.1523/ENEURO.0284-18.2019.

49. Pageler, N. M. *et al.* Effect of head orientation on gaze processing in fusiform gyrus and superior temporal sulcus. *NeuroImage* **20**, 318–329 (2003).
50. Jiang, J., Borowiak, K., Tudge, L., Otto, C. & von Kriegstein, K. Neural mechanisms of eye contact when listening to another person talking. *Social cognitive and affective neuroscience* **12**, 319–328 (2017).
51. Dikker, S. *et al.* Crowdsourcing neuroscience: inter-brain coupling during face-to-face interactions outside the laboratory. *NeuroImage* **227**, 117436 (2021).
52. De Jaegher, H., Di Paolo, E. & Gallagher, S. Can social interaction constitute social cognition? *Trends in cognitive sciences* **14**, 441–447 (2010).
53. De Jaegher, H., Di Paolo, E. & Adolphs, R. What does the interactive brain hypothesis mean for social neuroscience? A dialogue. *Philosophical Transactions of the Royal Society B: Biological Sciences* **371**, 20150379 (2016).
54. Di Paolo, E. A. & De Jaegher, H. The interactive brain hypothesis. *Frontiers in human neuroscience* **6**, 163 (2012).
55. Buschman, T. J. & Miller, E. K. Top-down versus bottom-up control of attention in the prefrontal and posterior parietal cortices. *science* **315**, 1860–1862 (2007).
56. He, B. J., Zempel, J. M., Snyder, A. Z. & Raichle, M. E. The temporal structures and functional significance of scale-free brain activity. *Neuron* **66**, 353–369 (2010).
57. Lakatos, P., Karmos, G., Mehta, A. D., Ulbert, I. & Schroeder, C. E. Entrainment of neuronal oscillations as a mechanism of attentional selection. *science* **320**, 110–113 (2008).
58. Haegens, S., Nácher, V., Luna, R., Romo, R. & Jensen, O. α-Oscillations in the monkey sensorimotor network influence discrimination performance by rhythmical inhibition of neuronal spiking. *Proceedings of the National Academy of Sciences* **108**, 19377–19382 (2011).
59. Canolty, R. T. *et al.* High gamma power is phase-locked to theta oscillations in human neocortex. *science* **313**, 1626–1628 (2006).

60. Liu, D. *et al.* Interactive brain activity: review and progress on EEG-based hyperscanning in social interactions. *Frontiers in psychology* **9**, 1862 (2018).
61. Tognoli, E., Lagarde, J., DeGuzman, G. C. & Kelso, J. S. The phi complex as a neuromarker of human social coordination. *Proceedings of the National Academy of Sciences* **104**, 8190–8195 (2007).
62. Kinreich, S., Djalovski, A., Kraus, L., Louzoun, Y. & Feldman, R. Brain-to-brain synchrony during naturalistic social interactions. *Scientific reports* **7**, 1–12 (2017).
63. Levy, J., Goldstein, A. & Feldman, R. Perception of social synchrony induces mother–child gamma coupling in the social brain. *Social cognitive and affective neuroscience* **12**, 1036–1046 (2017).
64. Mu, Y., Han, S. & Gelfand, M. J. The role of gamma interbrain synchrony in social coordination when humans face territorial threats. *Social Cognitive and Affective Neuroscience* **12**, 1614–1623 (2017).
65. Kingsbury, L. & Hong, W. A Multi-Brain Framework for Social Interaction. *Trends in Neurosciences* (2020).
66. Fletcher, P. C. *et al.* Other minds in the brain: a functional imaging study of "theory of mind" in story comprehension. *Cognition* **57**, 109–128 (1995).
67. Lombardo, M. V. *et al.* Shared Neural Circuits for Mentalizing about the Self and Others. *Journal of Cognitive Neuroscience* **22**, 1623–1635 (2010).
68. Pfeifer, J. H., Lieberman, M. D. & Dapretto, M. "I Know You Are But What Am I?!": Neural Bases of Self- and Social Knowledge Retrieval in Children and Adults. *Journal of Cognitive Neuroscience* **19**, 1323–1337 (2007).
69. Ruby, P. & Decety, J. Effect of subjective perspective taking during simulation of action: a PET investigation of agency. *Nature Neuroscience* **4**, 546–550 (2001).

70. Saxe, R., Moran, J. M., Scholz, J. & Gabrieli, J. Overlapping and non-overlapping brain regions for theory of mind and self reflection in individual subjects. *Social Cognitive and Affective Neuroscience* **1**, 229–234 (2006).
71. Saxe, R. & Powell, L. J. It's the Thought That Counts: Specific Brain Regions for One Component of Theory of Mind. *Psychol Sci* **17**, 692–699 (2006).
72. Müller, V., Sänger, J. & Lindenberger, U. Hyperbrain network properties of guitarists playing in quartet. *Annals of the New York Academy of Sciences* **1423**, 198–210 (2018).
73. Essl, M. & Rappelsberger, P. EEG cohererence and reference signals: experimental results and mathematical explanations. *Medical and Biological Engineering and Computing* **36**, 399–406 (1998).
74. Delorme, A. & Makeig, S. EEGLAB: an open source toolbox for analysis of single-trial EEG dynamics including independent component analysis. *Journal of neuroscience methods* **134**, 9–21 (2004).
75. Maris, E. & Oostenveld, R. Nonparametric statistical testing of EEG-and MEG-data. *Journal of neuroscience methods* **164**, 177–190 (2007).
76. Zalesky, A., Fornito, A. & Bullmore, E. T. Network-based statistic: identifying differences in brain networks. *Neuroimage* **53**, 1197–1207 (2010).
77. Nolte, G. *et al.* Robustly estimating the flow direction of information in complex physical systems. *Physical review letters* **100**, 234101 (2008).
78. Latora, V. & Marchiori, M. Efficient behavior of small-world networks. *Physical review letters* **87**, 198701 (2001).
79. Fortunato, S. Community detection in graphs. *Physics reports* **486**, 75–174 (2010).
80. Newman, M. E. & Girvan, M. Finding and evaluating community structure in networks. *Physical review E* **69**, 026113 (2004).
81. Newman, M. E. Mixing patterns in networks. *Physical review E* **67**, 026126 (2003).

82. Zhou, S. & Mondragón, R. J. The rich-club phenomenon in the Internet topology. *IEEE Communications Letters* **8**, 180–182 (2004).

83. Colizza, V., Flammini, A., Serrano, M. A. & Vespignani, A. Detecting rich-club ordering in complex networks. *Nature physics* **2**, 110–115 (2006).

Supplementary Files

This is a list of supplementary files associated with this preprint. Click to download.

- SupplementaryInformationfinal.docx
- SupplementaryInformationfinal.docx